The Giant Molecular Cloud Monoceros R2: 1. Shell Structure

Taoling Xie[1,2] and Paul F. Goldsmith[1,3]

1 Five College Radio Astronomy Observatory, Department of Physics and Astronomy, University of Massachusetts, Amherst, h4A 01003

2 Jet Propulsion Laboratory, California Institute of Technology, Pasadena, CA 91109

3 National Astronomy and Ionosphere Center, Cornell University, Ithaca, NY 14853-6801

Received ____________________; accepted ________________

Submitted to ApJ [illegible]

9/21/93

ABSTRACT

We have obtained a 45" resolution, Nyquist-sampled map in $CO\ J = 1 - 0$ covering approximately a 3° x 3° region of the giant molecular cloud Monoceros R2. The map consists of 167,000 spectra observed with the 15-clcIIlc:IIt focal plane array system on the FCRAO 14m telescope. The data r('veal that the large-scale structure of Mon R2 is dominated by a $\sim$ 30 pc diameter largely hemispherical shell containing $\sim 4 \times 10'^{1} M_{\odot}$ neutral material and expanding at $\sim 3 - 4\ km\,s^{-1}$ with symmetry axis roughly along the line of sight. The dynamical time scale of the shell is estimated to be $\sim 4 \times 10^{6}$ years, which is consistent with the age of main sequence stars powering the clusters of reflection nebulae in this region. There is no evidence for a red-shifted shell on the far side of the interior "bubble", which is largely devoid of molecular material. Distortions of the shell are obvious, suggesting inhomogeneity of the cloud and possible presence of a magnetic field prior to its formation. Dense clumps in Mon R2, including the main core and the GGD 12-15 core, appear to be condensations located 011 the large shell. The reflection nebulae with their illuminating stars as well as embedded 1 RAS sources suggest that triggered star formation has taken place over a large part of the Mon R2 shell, and thus may preferably lead to formation of massive stars.

Subject headings: ISM: clouds Reflection Nebulae Stars: ('ar]y-type -]]]] regions - ISM: structure - ISM: individual objects (Monoceros R2)

1. INTRODUCTION

Young stellar objects are born in molecular clouds in the Milky Way and external galaxies. Although the classification of these molecular clouds based on their morphological shapes and sizes is still ambiguous, the existence of giant molecular clouds (GMCs) and the fact that they arc the birth places of clusters of both low and high mass stars arc clear (cf. Blitz 1980; 1991; Shu, Adams & Lizano 19S7). The properties of stars and dusters of stars ought to be related to the initial density and other physical parameters of the clouds, but the violent dynamical effects of star forming processes may trigger subsequent generations of star formation (Blaauw 1964; 1991; Elmegreen & Lada 1977; Elmegreen 1992) as well as significantly altering the structure of the placental molecular cloud. Understanding the details of the relationship between young stars and clouds is an interesting theoretical and observational issue. A very useful tracer of the morphological and kinematic structure of GMCs is CO $J = 1-0$ emission, but the large angular sizes of this type of clouds make it difficult to obtain such maps with proper sampling and resolution.

Mon R2 is a typical GMC with a mass of a few $10^4 M_\odot$ and a size of some 30 x 50 pc (Kutner & Tucker 1975; Maddalena *et al.* 1986), which harbors two relatively well studied star forming condensations, the main core (cf. Beckwith *et al.* 1976; Loren 1977; Wolf *et al.* 1990) and GGD 12-15 (cf. Cohen & Schwartz 1980; Little *et al.* 1990). At a distance of $D = 830$ pc and a galactic latitude of 12°, this GMC is associated with numerous reflection nebulae distributed in a narrow E-W oriented band across the cloud, most of which are illuminated by A and B type main sequence stars (Herbst & Racine 1976; hereafter HR). Hughes & Baines (1985) suggested that star formation Has been taking place in a line or an annular ring on the scale of the GMC. However, molecular data then available allowed only a morphological study of the structure of Mon R2 on a large scale.

2. OBSERVATIONS

We have made observations of $CO\ J = 1-0$ emission from Mon R2 using the QUARRY 15-element focal plane array on the 14 m FCRAO telescope in New Salem, Massachusetts between 1991 April and 1992 January. A detailed description of the receiver system can be found in Erickson *et al* (1 W?). The mapping was centered on $\alpha(1950) = 06^h05^m22^s$, $\delta(1950) = -06°22'25''$, the position of the infrared star cluster in the main core of Mon R2 (Beckwith *et al* 1976). The spacing of the data was 25", the FWHM beam size of the telescope about 45" at 115 GHz, and the main beam efficiency $\simeq$ 0.45. A 32 channel filterbank with velocity resolution 0.65 $km\ s^{-1}$ centered on $V_{LSR} = 9.9\ km\ s^{-1}$ was used with each of the 15 receivers. Chopper wheel calibration was used and the data were taken in a position-switching mode with a common reference position at $\alpha(1950) = 06^h11^m00^s$, $\delta(1950) = -04°30'00''$. This position was verified to be free of $^{12}CO\ J = 1-0$ emission to an rms noise of 0.05 K using positional switched measurements between this position and a second reference position several degrees away. The single side-band system temperature of the system ranged from $\sim 650\ K$ to $\sim 1600\ K$, and integration times were adjusted in order to yield a rms noise level of $\sim 0.5K$.

3. SHELL STRUCTURE

3.1. Morphological and Kinematic Evidence

Figure 1 (plates) presents the velocity channel maps for $^{12}CO\ J = 1-0$ emission. The outline of the gas emission in general agrees with the boundaries of the regions with large optical extinction (Kutner & Tucker 1975), which were roughly divided into several dark clouds denoted L1643, L1644, L1645 and L1646 (Lynds 1962; POSS overlay 1979; Dixon

& Sonneborn 1980). The general morphology seen in Figure 1 is also consistent with that revealed by the ^{12}CO $J = 1 - 0$ map of Maddelena *et al.* (1986), which has a resolution of 8.7' and a sampling interval of 15' or 30'. The strongest emission occurs in the main core at $\alpha(1950) = 06^h05^m22^s$, $\delta(1950) = -06°22'25"$, where active star formation has been taking place in the dense gas traced by millimeter transitions of molecules such as CS, HCO^+, and HCN (Xie 1992). This core contains a group of reflection nebulae, a compact HII region, a massive bipolar outflow and an H_2O maser (Loren 1977; 1981; Bally & Lada 1983). Roughly 45' to the east of this core, there appears a second strong source, the GGD 12-15 region, which coincides with another small group of reflection nebulae, a compact HII region, a bipolar outflow and a H_2O maser (cf. Harvey *et al.* 1985; Little, Heaton & Dent 1990). The most striking feature related to the bipolar outflows is the "eggplant-shaped" shell extending some 30' to the northwest of the main core (Xie, Goldsmith, & Patel 1993). There is also a velocity gradient along the SE-NW elongation of the cloud, as as noticed by Maddelena *et al.* (1986). This velocity gradient is consistent with the direction of the galactic plane and the magnetic field (Dyck & Lonsdale 1979), but its sense is opposite to that expected from galactic rotation (Hughes & Baines 1985).

There are two conspicuous features that have either escaped the attention of previous investigators or not been revealed by existing data. First, in the western portion of the cloud, there appears a strikingly sharp **N-S** oriented ridge of emission, most evident in high velocity channels shown in Figure 1. There is also a roughly east-west oriented emission ridge in the eastern portion of the cloud including the GGD12-15 region and a chain of other cores on the ridge. The sharpness and cleanness of the edge of the emission ridges suggest that they are caused by fairly recent dynamical events and may be the results of shock compression of the molecular gas. The ridges appear corrugated, suggesting kinematic instability of shock front development (Elmegreen 1992).

The second feature suggestive of a dynamical event is the ^{12}CO $J = 1 - 0$ emission at, some intermediate velocities (V_{LSR} = 10.21 - 12.18 $km\ s^{-1}$) which shows a ring-like morphology on a scale of tens of arcminutes (most conspicuous at V_{LSR} = 10.88 $km\ s^{-1}$). Despite the fact that the GGD 12-15 core falls inside this feature and that this ring does not have a uniform intensity and is somewhat broken in the northern side, the ring feature is clearly present and seem to be roughly centered on a small group of reflection nebulae at $\alpha(1950) = 06^h07^m$, $\delta(1950) = -06°1i$" (NGC2182 region, Kutner & Tucker 1975; HR).

In addition to the morphological "ring" feature described above, there is also a systematic variation of the gas velocity with position. At low LSR velocities the gas emission shows very wispy features and is concentrated mainly in the central part and at the SE corner of the cloud. At higher velocities the gas emission is concentrated in the outer part of the region mapped, along the N-S emission ridge, and in the NW corner. It is clear that this velocity variation cannot be explained merely in terms of the SE-NW velocity gradient mentioned above.

The morphological ring and the velocity variation are not isolated. This can be better seen in Figure 2, which shows spatial-velocity diagrams along east-west cuts through the main core and the GGD 12-15 core. Along both cuts the gas in the inner part of the cloud is blue-shifted relative to the gas in the outer parts (eastern and western extremes of the cloud), forming a blue-shifted bow-shaped feature in the spatial-velocity diagrams. The spatial extent of this bow-shaped feature is $\sim$ 110', which corresponds to 26.5 pc at a distance of 830 pc (HR). Despite their large size, the arc-shaped features in the S-V diagrams appear relatively smooth and continuous, which makes a chance superposition of gas at different velocities along the line of sight an implausible explanation. The maximum velocity displacement of the blue-shifted gas relative to the outer ambient emission is $\sim 3 - 4\ km\ s^{-1}$. The uncertainty in this estimate results primarily from the determination of an average velocity for the gas in the outer region of the cloud. The dynamical time scale for the shell structure is thus $\sim 4 \times 10^6$ years.

3.2. A Highly-Simplified Model

While many conceivable physical processes may give rise to velocity variations over a large scale in a GMC, few could give rise to the smooth change of velocity with position and the continuousness of the emission exhibited by the Mon R2 shell. The simplest and most attractive explanation is provided by a hemispherical or "}vok-like" expanding shell. The projected center of the shell is close to the NGC 2182 region. Figure 3 presents a cartoon of this simplified model. Assuming the shell to be thin and the velocity dispersion of the gas to be small, the expected gas velocity along a line of sight can be expressed as

$$V(x) = V_0(1 - \frac{x^2}{r_0^2})^{1/2}, \quad (1)$$

where V_0 is the radial velocity, r_0 is the radius and x is the projected distance from the projected c.enter in the plane of sky. The continuous, smooth arc-shaped features seen in Figure 2 gives $V_0 = 3 - 4\ km s^{-1}$, and $r_0 = 55'$ (13 pc at a distance of 830 pc). In this simple model, the velocity in the outer part of the cloud is assumed to be the original cloud velocity, and the axis of symmetry of the shell lies roughly along the line of sight.

Of particular interest are the morphology and location of the two dense cores (the main core and GGD 12-15 core), with respect to the shell structure. Projected inside the large ring-feature mentioned above, GGD 12-15 shows a sharp roundish edge (see e.g. Figure 1 at V_{LSR} = 10.23- $10.88 km\, s^{-1}$) facing the projected geometrical center of the ring, reminiscent of the bow-shaped head of cometary globules (cf. Reipurth 1 983; Elmegreen 1992; Patel, Xie & Goldsmith 1993). While the main core seems to be part of the ring feature at V_{LSR}= 10.23- 10.SSk7n s" 1 , it falls into the cavity on the eastern side of the N-S ridge seen in the maps for V_{LSR} larger than 11 km s^{-1}. The velocities of the gas in the main core and the GGD 12-15 core relative to the gas in the shell are best seen in Figure 2. The self-absorption dip of the ^{12}CO $J = 1 - 0$ line profiles and the high velocity wings due to the bipolar outflow somewhat complicate the S-V diagram, but the gas in the main core shows up as a coherent part of the blue-shifted bow-shaped feature in the S-V diagrams. This is most easily understood if the main core is located on the expanding shell moving towards us. In the case of GGD 12-15, the $^{12}CO\ J = 1 - 0$ self-reversal and complicated velocity variations of the surrounding make this interpretation less convincing, but we feel that it is safe to conclude that this region is a shocked clump of gas associated with the large-scale shell structure.

A simple hemispherical or a wok-like shell model cannot offer satisfactory explanations for all the features revealed by the high resolution $^{12}CO\ J = 1 - 0$ images in Figure 1. S-V diagrams along different cuts are not always as simple as suggested by Figure 2. The emission in many is more fragmented, although the general arc-shaped feature is generally apparent. In fact, distortions of the shell structure are clearly demonstrated by the emission ridges which run almost, all way across the cloud, and the open side of the ring structure in the NW corner of the map. The overall cloud is somewhat asymmetric being $\sim$ 30 pc east-west by 45 pc north-sourth (Maddelena 1986). However, a hemispherical expanding shell seems to be a simple and satisfactory first-order model of the large scale structure of Mon R2.

3.3. Kinetic Energy

It is not easy to make an accurate calculation of the kinetic energy of the expanding motions because it requires the determination of a reference velocity, which is model-dependent. But if one makes an assumption that a large proportion of the cloud mass is being swept into an expanding shell and the geometry of the shell is hemispherical, then the energy in three dimensions in the expansion is given by $E = 1/2\,M(\Delta V)^2 \sim 6 \times 10^{48}$ ergs, where the cloud mass M is taken to be the 1,'1'1'; mass of $4 \times 10^4\ M_\odot$ (obtained from

$^{13}CO\ J=1-0$ data as discussed by Xie (1992)) contained in the shell, and the shell expansion velocity ΔV is taken to be $4\ km\ s^{-1}$. Various possible uncertainties are involved in this estimate, including deviations from hemispherical geometry, other components of systematic motion (including bipolar outflows in cores) and uncertainties in the mass actually associated with the shell.

Another way to estimate the total kinetic energy is to calculate the kinetic energy for each pixel of the map using the $^{12}CO\ J=1-0$ and $^{13}CO\ J=1-0$ data under the assumption of LTE (Xie 1992), and then to sum over the whole shell. This procedure gives an estimate of $1 \times 10^{49}\ ergs$ which includes the "kinetic energy" due to turbulence and other motions. But it is important to note that this estimate of kinetic energy is only for one dimension - along the line of sight. Given the various uncertainties and the difficulties, we feel that the total kinetic energy of the systematic motions of the large-sdc expanding shell is likely to be in the range 5 - 20 $\times 10^{48}$ ergs.

4. TRIGGERED STAR FORMATION IN MON R2

HR first hinted that there are at least two generations of star formation in Mon R2. One generation, represented by the many A and B type main-sequence stars associated with reflection nebulae, occured at least 6 million years ago (the age of the cluster, HR), consistent with the dynamical time scale of the shell discussed in this paper. The second generation is the ongoing star formation in the cores and in the shock-compressed gas in the ridges as traced by the bipolar out flows, compact HII regions, H_2O masers and IRAS point sources with an age of probably only 10^4 --- 10^5 years (Beckwith *et al.* 1976; Loren 1977; Xie 1992). The distribution of the reflection nebulae and the IRAS point sources with respect to the gas can be seen in Figure 1. The majority of IRAS point sources, which are likely young stellar objects still embedded in dust and gas, are concentrated near the sharp emission ridges. Particularly striking is a group of IRAS point sources located on the N-S emission ridge, whose distribution closely follows the extension of strongest emission to the north. This coincidence of IRAS point sources with clumped and high density gas emission, combined with the evidence for the existence of large shell structure and the expected shock activity, strongly suggests that shock compression of the gas may have triggered the current generation of star formation. The detailed structure of the shell and a discussion of triggered star formation in Mon R2 will be presented in a subsequent paper (Xie & Goldsmith 1993).

TX thanks his PhD thesis committee members, Ed Chang, Bob Dickman and Ron Snell for exceptionally good service. Useful discussions with Giles Novak, Tom Jarrett, John Kwan, Steve and Karen Strom, Bill Langer and Nimesh Patel are gratefully acknowledged. This work is partly supported by NASA grant NAG 5-1363 and NSF grant AST 88-15406.

AUTHORS' ADDRESSES:

Paul F. Goldsmith: National Astronomy and Ionosphere Center, Cornell University, Space Sciences Bldg., Ithaca, NY 14853-6801

Taoling Xie: MS 169-506, JPL/Caltech, Pasadena, CA 91109

Figure Captions

Figure 1. $^{12}CO\ J = 1 - 0$ channel maps of Mon R2. Each panel displays the $^{12}CO\ J = 1 - 0$ emission within a velocity width of 0.65 $km\,s^{-1}$, and the centroid velocity is indicated in the upper left corner of each panel. Also shown in the maps are the IRAS point sources (solid stars), reflection nebulae (solid squares) and HII regions (open squares) as discussed in Xie (1 992).

Figure 2. (a) A S-V diagram in Right Ascension, going through the center of the main core at $\delta = -06°22'25"$. (b) A S-V diagram in Right Ascension going through the center of the GGD 12-15 core at $\delta = -06°10'40"$. The contour levels are 0.7, 1.4, ... 14 K.

REFERENCES

Bally, J. & Lada, C.J. 1983, *ApJ, 265*, 824

Beckwith, S., Evans II, N. J., Becklin, E.E., & Neugebauer, G. 1976, *ApJ, 208*, 390

Blaauw, A. 1964, *ARA&A, 2*, 213

Blaauw, A. 1991, *The Physics of Star Formation and Early Stellar Evolution*, ed. C.J. Lada & N.D. Kylafis (Dordrecht:Kluwer), 125

Blitz, L., 1980, in *Giant Molecular Clouds in the Galaxy*, eds. P.M. Solomon and M.S. Matthews (Tucson: University of Arizona Press), 201

Blitz, L. 1991, *The Physics of Star Formation and Early Stellar Evolution*, ed. C.J. Lada & N.D. Kylafis (Dordrecht:Kluwer), 3

Cohen, M., & Schwartz, R.D. 1980, *MNRAS, 191*, 165

Dixon, R.S., & Sonnenborn, G. 1980, Master List of Nonstellar Optical Objects, Ohio State University Press

Dyck, H.M., & Lonsdale, C.J. 1979, *AJ, 84*, 1339

Elmegreen, B.G. 1992, preprint, *III Canary Islands Winter School*, to be published by Cambridge University Press

Elmegreen, B.G., & Lada, C.J. 1977, *ApJ, 214*, 725

Erickson, N.R., Goldsmith, P.F., Novak, G., Grosslein, R. M., Viscuso, P.J., Erickson, R.B., & Predmore, C.R. 1992, *IEEE Trans. on Microwave Theory and Techniques, 40*, 1

Harvey, P.M., Wilking, B.A., Joy, M. & Lester, D.F. 1985, *ApJ, 288*, 725

Herbst, W., & Racine, R. 1976, *AJ*, 81, 840

Hughes, V.A., & Baines, J.G.N. 1985, *ApJ, 289*, 238

Kutner, M.L., & Tucker, K.D. 1975, *ApJ, 199*, 79

Little, L.T., Heaton, B.D., Dent, W.R.F. 1990, *A&A*, 232, 173

Loren, R.B. 1977, *ApJ, 215*, 129

Loren, R.B. 1981, *ApJ, 249*, 550

Lynds, B.T. 1962, *ApJS, 7*, 1

Maddalena, R. J., Morris, M., Moscowitz, J., & Thaddeus, P. 1986, *ApJ, 303*, 375

Patel, N., Xie, T., & Goldsmith, P.F. 1993, to appear in *ApJ*

Reipurth, B. 1983, AA, 117, 183

Shu, F.H., Adams, F. C., & Lizano, S. 1987, *ARAA, 25*, 23

Wolf, G. A., Lada, C.J., & Bally, J. 1990, *AJ, 100*, 1892

Xie, T. 1992, PhD thesis, University of Massachusetts at Amherst

Xie, T., Goldsmith, P. F., & Patel, N, 1993, *ApJ, in* press

Xie, T., & Goldsmith, P.F. 1993, in preparation.

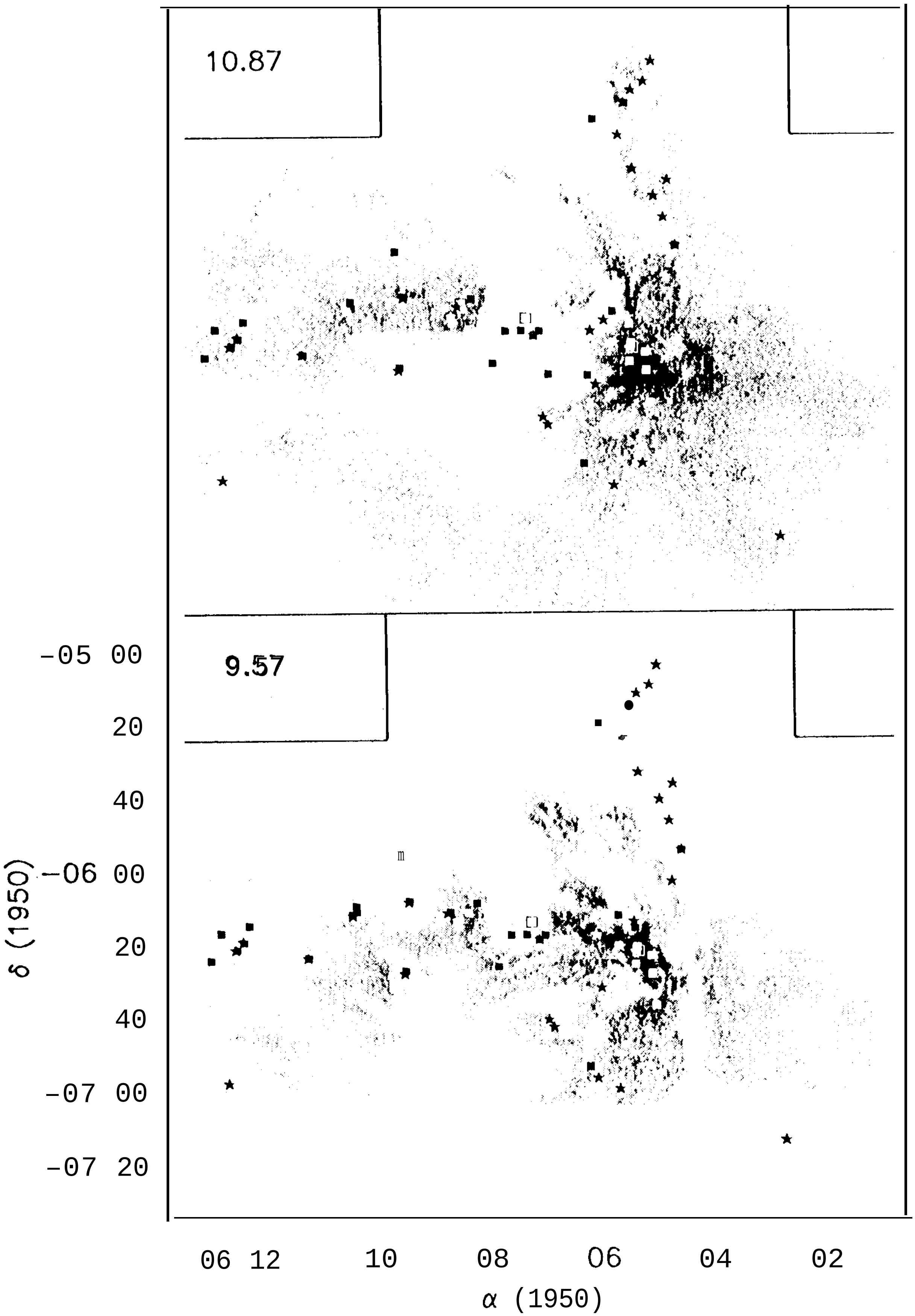
10.87
9.57
−05 00
20
40
−06 00
20
40
−07 00
−07 20
δ (1950)
06 12
10
08
06
04
02
α (1950)

Fig. 1

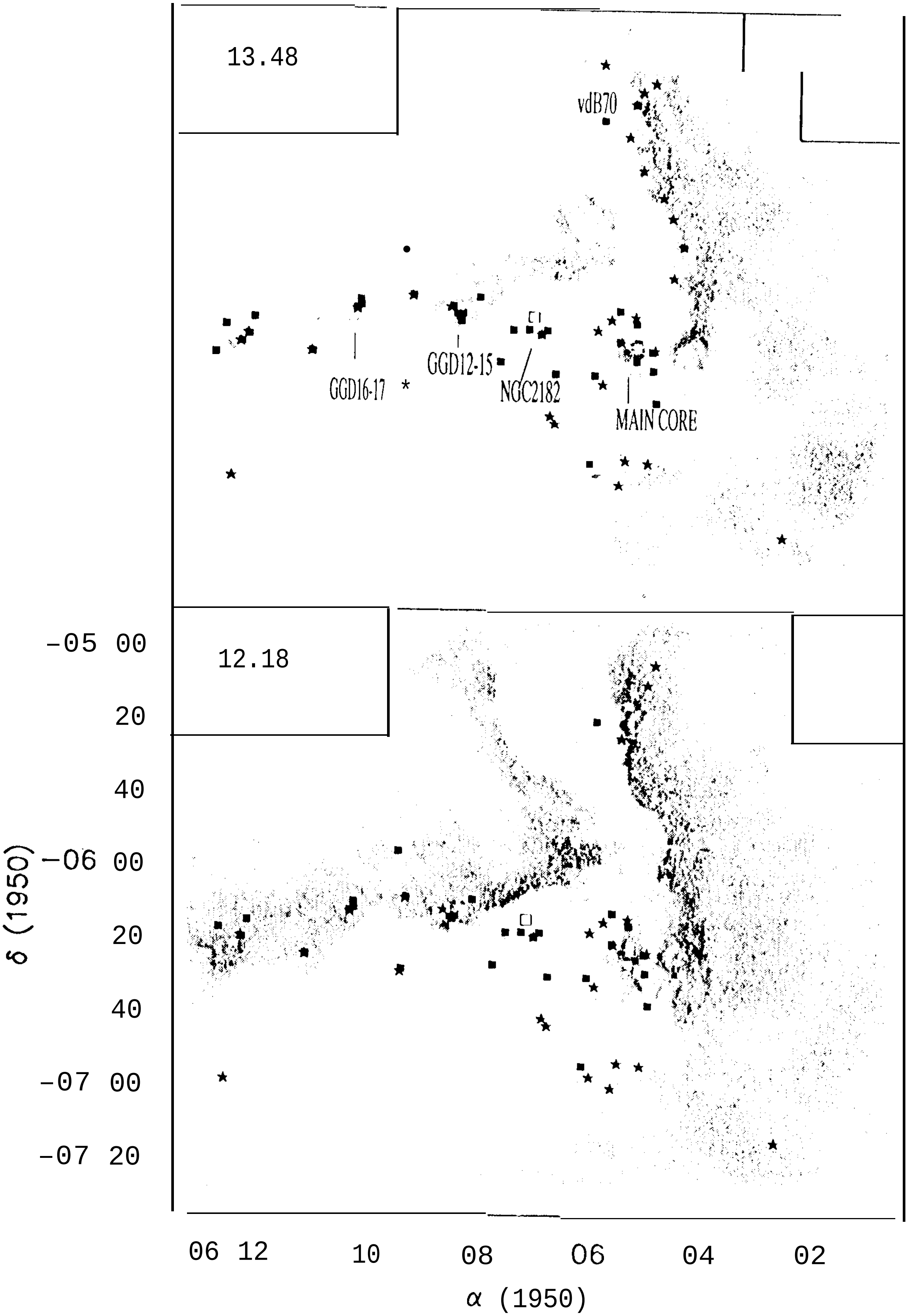
13.48
vdB70
GGD16-17
GGD12-15
NGC2182
MAIN CORE
12.18
−05 00
20
40
−06 00
20
40
−07 00
−07 20
δ (1950)
06 12
10
08
06
04
02
α (1950)

Fig 1b

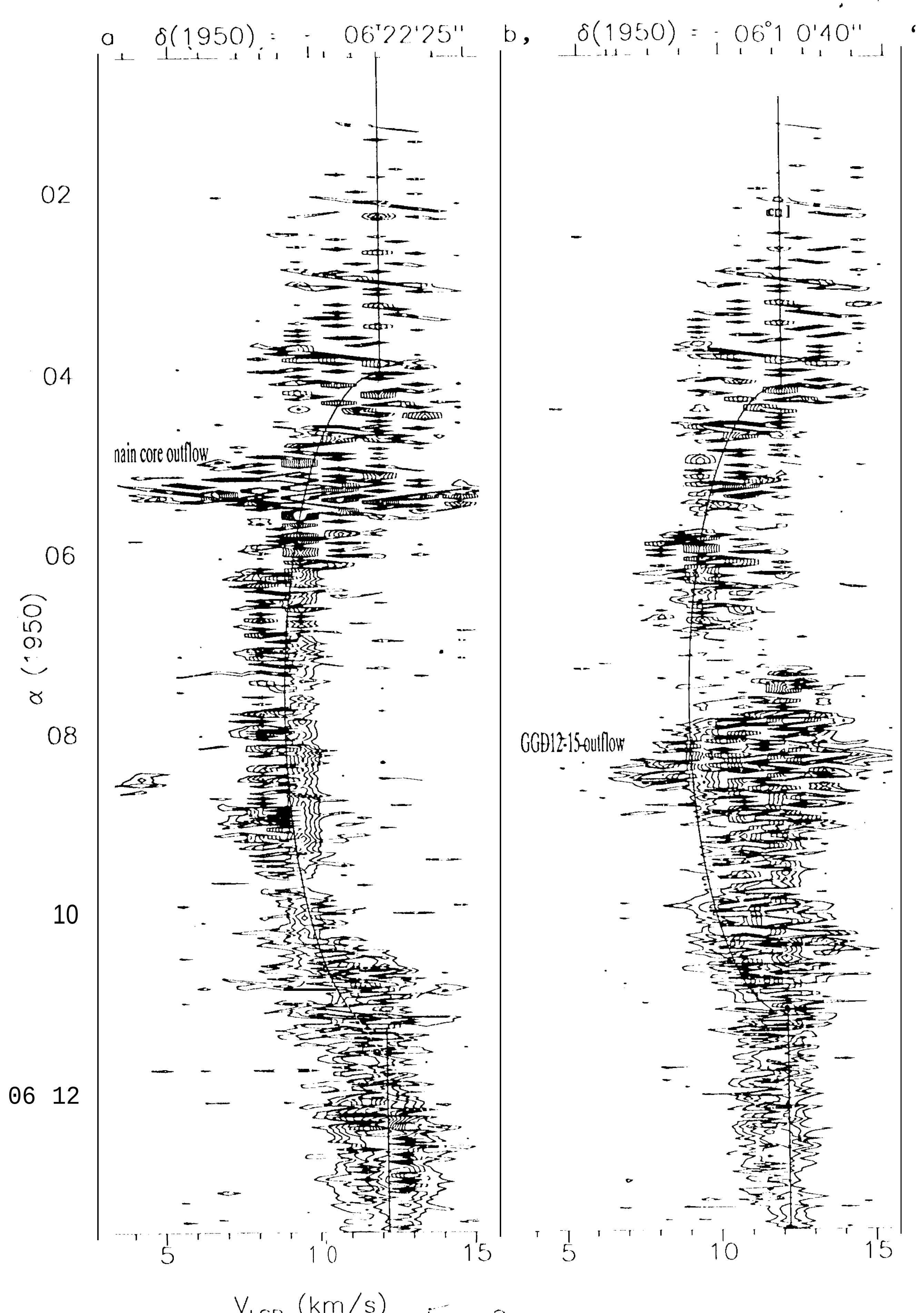
a δ(1950) = - 06°22'25"
b, δ(1950) = - 06°10'40"
02
04
06
α (1950)
08
10
06 12
nain core outflow
GGD12-15-outflow
5
10
15
V_{LSR} (km/s)

Fig 2